Journal of Materials Chemistry A

Facile New Approach to High Sulfur-Content Materials and Preparation of Sulfur-Lignin Copolymers

Journal:	*Journal of Materials Chemistry A*
Manuscript ID	TA-COM-09-2019-010742.R2
Article Type:	Communication
Date Submitted by the Author:	09-Dec-2019
Complete List of Authors:	Karunarathna, Menisha; Clemson University, Department of Chemistry Tennyson, Andrew; Clemson University, Department of Chemistry Smith, Rhett; Clemson University, Department of Chemistry

COMMUNICATION

Facile New Approach to High Sulfur-Content Materials and Preparation of Sulfur-Lignin Copolymers

Menisha S. Karunarathna,[a] Andrew G. Tennyson,[ab] and Rhett C. Smith,[*a]

Received 00th January 20xx,
Accepted 00th January 20xx

DOI: 10.1039/x0xx00000x

This report introduces a new approach to high sulfur-content materials. This route, RASP (radical-induced aryl halide / sulfur polymerization), expands the substrate scope beyond olefins required for the traditional inverse vulcanization route to such materials. RASP allows direct reaction of two unmodified industrial waste products to give lignin-sulfur composites.

High sulfur-content materials are at the forefront of sustainable material science because they can be thermally healable[1-7] and are sometimes so environmentally compatible that they can even be used as fertilizers.[8, 9] Elemental sulfur, itself an industrial waste product, comprises the primary component of such materials,[6, 10] many of which can be made by direct reaction of sustainably-sourced olefin comonomers with sulfur.[11-13]

Inverse vulcanization, whereby olefins react with thermally-generated polymeric sulfur radicals (Scheme 1A), is the preeminent route to high sulfur-content materials.[12, 14-16] Whereas inverse vulcanization is an exceptional route for copolymerization of sulfur with sustainably-sourced olefins, the most abundant biomass feedstocks such as lignin and cellulose lack olefin moieties and must be derivatized to react via inverse vulcanization.[17, 18] Unfortunately, olefination / purification / separation detracts significantly from the greenness, atom economy and affordability of such processes. A more sustainable and atom economical process to valorise lignocellulosic waste for high sulfur-content materials could be a meaningful advance towards a biorefinery-driven green economy.

Herein we introduce a new route to high sulfur-content materials: radical-induced aryl halide / sulfur polymerization (RASP, Scheme 1B). RASP utilizes an aryl halide comonomer and thus expands the scope of viable monomers beyond olefins that can be polymerized by inverse vulcanization.

A). Inverse Vulcanization (*Pyun, 2013*): *Employs an Olefin with Majority Sulfur*

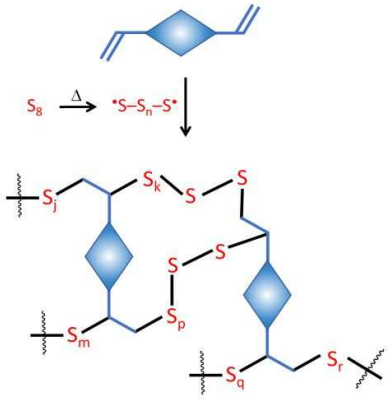

B). RASP (*This Work*): *Employs an Aryl Halide with Majority Sulfur*

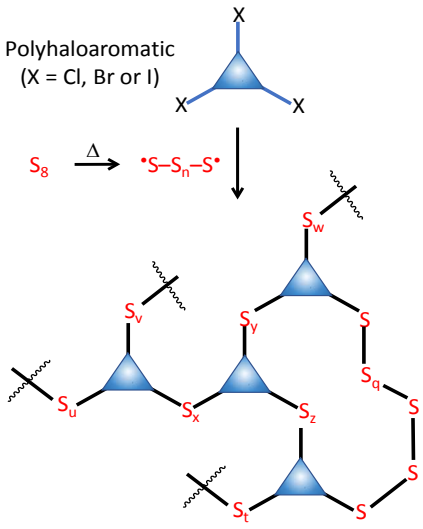

Scheme 1. Established (A) and new (B) routes to high sulfur-content materials

[a] *Department of Chemistry , Clemson University, Clemson, South Carolina, 29634, United States*
[b] *Department of Materials Science and Engineering, Clemson University, Clemson, South Carolina, 29634, United States*

†Electronic Supplementary Information (ESI) available: Proton NMR spectral data, FTIR spectra, TGA curves, analysis of char yield versus composition; DSC curves.

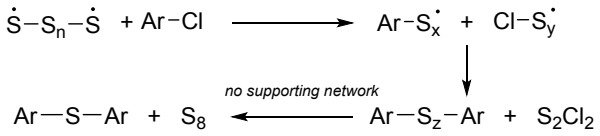

Scheme 2. The reaction of aryl chlorides with elemental sulfur initially generates polysulfur-bridged aryls that, in the absence of a supporting network, subsequently degrade to diallylsulfide

Mechanistically, inverse vulcanization is a modification of Goodyear's vulcanization in which sulfur serves is the majority component (Scheme 1A). The RASP approach (Scheme 1B) likewise mirrors an established industrial process, carbonate-free Macallum polymerization, but using majority component sulfur. Macallum polymerization is the established industrial route to polysulfides (in which only a single sulfur atom lies between aryl groups in the backbone) and so, like vulcanization, has demonstrated commercial scalability.[19]

The established mechanism by which elemental sulfur reacts with aryl chlorides at ≥180 °C (Scheme 2) involves halide atom abstraction followed by formation of oligo- or polysulfide-bridged aryl rings.[20] Such polysulfide catenates relax to monosulfide bridges with extrusion of sulfur as the orthorhombic (S_8 rings) allotrope during or shortly following reaction. Polymeric sulfur can, however, be stabilized by a supporting crosslinked network. The lignin/sulfur network formed by inverse vulcanization in **SAL$_{95}$** (Scheme 3A), for example, stabilizes polymeric sulfur chains averaging 48 sulfur atoms in length.[17] It was thus hypothesized that chlorolignin/sulfur networks prepared by RASP could likewise support network-stabilized polymeric sulfur domains.

Valorisation of lignin remains a significant challenge in sustainability science, especially given that lignin product value is often a limiting economic factor in biorefinery processes. Pulp bleaching produces chlorolignin at a rate of about 60 Mt/y, a major source of toxic anthropogenic chlorinated organics in the environment.[21] Recovering and developing useful purposes for industrial waste lignin/chlorolignin are thus imperative goals for a sustainable green economy. Chlorolignin was thus selected as the most impactful substrate for testing RASP.

The chlorolignin subjected to RASP in this study was derived from a softwood alkali lignin typical of that present in pulp waste. Lignin is a complex biopolymer made up of a variety of potential structural units[22] (Table S1 & Figure S1 in the ESI for quantification of composition of lignin used herein).[23-25] Chlorolignin (8.75 wt.% Cl from elemental analysis) was prepared by reaction of lignin with $NaClO_3$(aq) at room temperature. The only stoichiometric side products of this reaction are NaCl and H_2O, making this an attractive approach to produce chlorolignin from agricultural waste streams or biorefinery lignin as well. Chlorination was evident from elemental analysis and strong IR peaks of C–Cl deformation[26] observed at 493 and 577 cm^{-1} and concomitant decrease in intensity and shifting of the aromatic mode from 1512 cm^{-1} to 1496 cm^{-1} (Figure S2, ESI).[27]

A polymerization temperature of 230 °C was selected based on temperature-dependence studies on polysulfide formation from aryl halides.[28] Lignin does not exhibit appreciable reaction with sulfur at this temperature: *chlorination is necessary for RASP*. Several copolymers of chlorolignin and sulfur (**CLS$_x$**, *x* = wt.% sulfur, varied from 80-99), however, were readily prepared by simply heating the two comonomers together under nitrogen. **CLS$_x$** copolymers are dark solids that are readily remeltable simply by heating above 140 °C and the molten samples can be poured into moulds to create various shapes (Figure 1).

Whereas preparation of **SAL$_{95}$** by inverse vulcanization (Scheme 1) suffered from significant immiscibility of lignin and sulfur such that a maximum of 5 wt.% lignin could be incorporated,[17] sulfur and chlorolignin were fully miscible at 230 °C, so nearly all of the chlorolignin in the monomer feed (up to 19 wt.%) was incorporated into **CLS$_x$**. This was confirmed by elemental analysis (Table S3 in the

A)

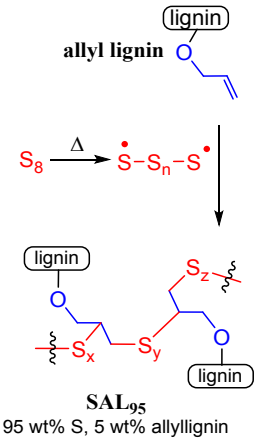

B)

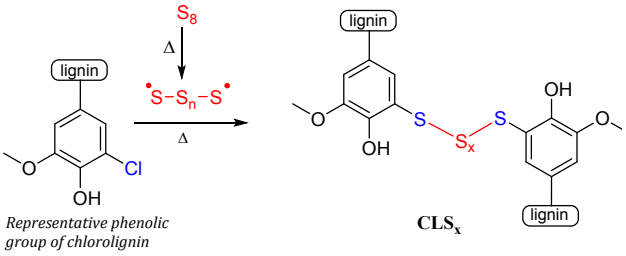

Scheme 3. A) Inverse vulcanization of allyl lignin produces crosslinked networks comprising stabilized polymeric sulfur domains. In **SAL$_{95}$**, the average polysulfide crosslink is 48 sulfur atoms long. B) RASP of chlorolignin to form **CLS$_x$**. In **CLS$_x$**, the average polysulfide crosslinks are 12-31 S atoms in length.

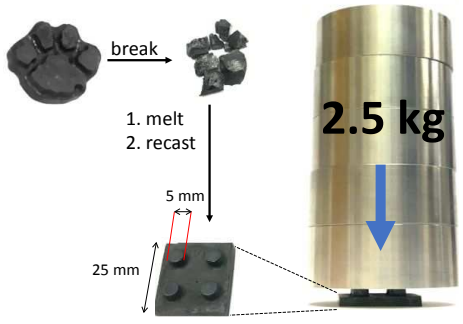

Figure 1. Photos of **CLS$_x$** materials illustrating their appearance, remeltability and qualitative strength of small cast items.

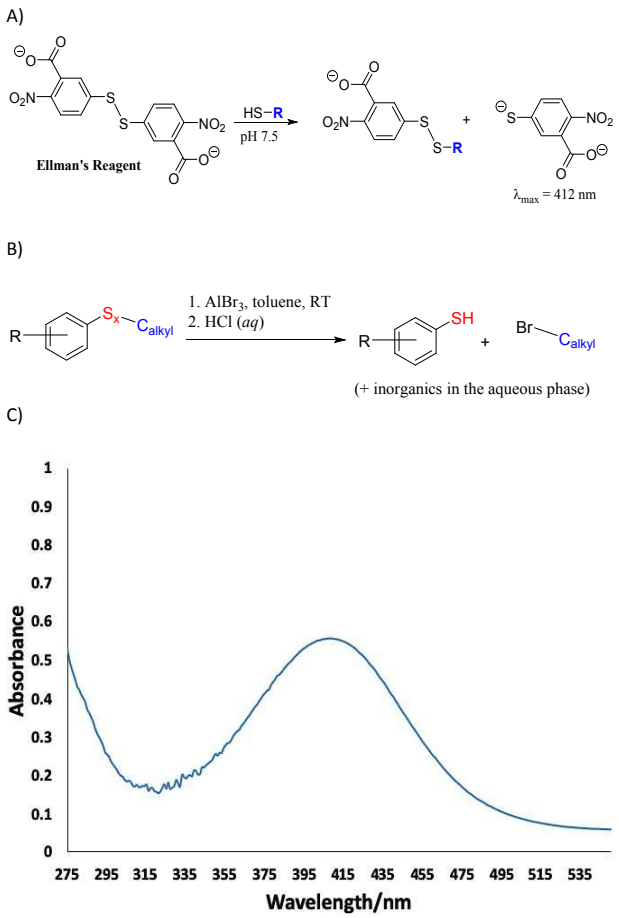

Figure 2. A) Reaction of $AlBr_3$ with sulfur-crosslinked organics leads to cleavage of S–C_{alkyl} bonds but not of S–C_{aryl} bonds, giving alkyl bromides and aryl thiols. B) The reaction of thiols with Ellman's reagent produces a selective colorimetric response, producing a compound having an absorption maximum of 412 nm. C) The UV-vis spectrum of **CLS_{80}** depolymerization products showing a positive result for aryl thiols after exposure to Ellman's reagent.

supporting information). In the RASP mechanism (Scheme 2), chlorine is removed as S_2Cl_2. The S_2Cl_2 is quite reactive, however, and is expected to react with the abundant alcohol functionalities in the lignin backbone (a reaction that takes place readily even at –95 °C) to form HCl and mixtures of ROSSOR, RO(SO)OR, and ROSSOR, which may themselves degrade to other species at the elevated reaction temperature.[29]

Formation of C–S bonds in **CLS_x** was confirmed by the emergence of a peak at 605–619 cm^{-1} (C–S stretch)[17, 30] in the infrared spectra (Figure S3, ESI). The proposed *aryl*-sulfur bond formation was unequivocally confirmed by analysis of depolymerization products as follows. **CLS_x** samples were first depolymerized by reaction with $AlBr_3$. Aluminium tribromide reacts with S–C_{alkyl} bonds to produce Br–C_{alkyl} bonds, but the S–C_{aryl} bonds remain intact, producing aryl thiols after aqueous workup (Figure 2A).[31, 32] In this way, the only thiols in the depolymerization mixture result from S–C_{aryl} bonds in the polymer. Analysis of thiols by Ellman's reagent leads to a species absorbing at ~412 nm, so that thiol content can be assessed by UV/vis spectroscopy (Figure 2B).[33, 34] Prior to depolymerization, **CLS_x** tests negative for thiols, suggesting few if any surface –SH moieties are present. After depolymerization, however, the depolymerization products tested positive for thiols, as manifest by the emergence of a strong peak with λ_{max} = 409 nm in the UV/vis spectrum (Figure 2C), thus confirming S–C_{aryl} bond formation as proposed. Although most of the organic fragments from depolymerization are expectedly too heavy to detect in GC-MS analysis, we were able to identify tolyl thiol and ditolylsulfide by this analysis, further confirming S–C_{aryl} bond formation and crosslinking of aryl rings in the product (Figure S12, ESI).

Previous high sulfur-content materials of sulfur with cellulose/lignin produced by inverse vulcanization are composites comprised of sulfur-crosslinked networks wherein some of the voids contain CS_2-extractable free sulfur. CS_2-fractionation of **CLS_x** likewise allowed quantification of covalently bound versus free sulfur and thus calculation of the average length of oligosulfur crosslinks in **CLS_x**. This analysis revealed that the average crosslink consists of 12-31 sulfur atoms, somewhat shorter than the average crosslink length of 48 sulfur atoms in **SAL_{95}**. This is expected because higher lignin percentages expectedly correlate with higher crosslink density and thus shorter average crosslink lengths.

Thermogravimetric analysis (TGA) was employed to assess the thermal stability of **CLS_x** compared to orthorhombic sulfur and lignin. Whereas orthorhombic sulfur exhibits a single decomposition process with a decomposition temperature (T_d) at 228° C, lignin decomposes over a broad temperature range[35] characterized by two primary decomposition events at 201 °C (degradation of propanoid side chains) and at 360–370 °C (cleavage of β-β and C–C linkages). Chlorolignin shares many of the same thermal decomposition features of lignin. Following some water removal from 90-100 °C, a broad degradation was observed starting at 201 °C and continuing gradually up to 450 °C. Eventually, chlorolignin lost 47 wt.% of its initial mass, leaving a 53% char yield at 800 °C under N_2. Given that **CLS_x** materials are 80-99 wt.% sulfur, it is unsurprising that their initial thermal decomposition resembles that of sulfur (Figure S5, ESI).[1, 36 17, 18] The char yield (remaining mass after heating to 800 °C) of highly aromatic polymers like lignin is generally quite high. The char yield of **CLS_x** thus increases linearly with the wt % of lignin incorporated (Figure S6 in the supporting information).

Differential scanning calorimetry (DSC) revealed that only higher chlorolignin content materials (**CLS_{80}**, **CLS_{90}**, and **CLS_{95}**) show endothermic peaks at −35 to −41 °C, corresponding to the characteristic glass transition for polymeric sulfur.[37, 38] **CLS_x** samples also showed cold crystallization exotherms ranging from 21 to 23 °C and 43 to 46 °C attributable to partial organization of polymeric sulfur domains within the composite (Figure S7 in the supporting information).[39] These peaks confirm that the polymer networks prepared by RASP stabilize polymeric sulfur domains in a manner similar to networks prepared by inverse vulcanization, which exhibit similar features in DSC analysis.[17] Each of the samples also exhibited a melting temperature (T_m) of 117–120 °C attributable to the aforementioned CS_2-extractable orthorhombic sulfur in the materials. Importantly, none of the DSC data for **CLS_x** samples showed features for lignin or chlorolignin domains separate from the crosslinked network.

The percent crystallinity (Table 1) of **CLS_x** relative to crystalline orthorhombic sulfur was also readily calculable from DSC data using integrations of melting and cold crystallization enthalpies (Table 2).

Table 1. Thermal analysis of **CLS$_x$** materials

Materials	$T_d^{[a]}$ /°C	Cold crystallization peaks/ °C	$T_m^{[b]}$/°C	ΔH_m J/g	ΔH_{cc} J/g	Percent crystallinity[c]
CLS$_{80}$	238	-4, 39	117	30	12	36
CLS$_{85}$	237	-10, 35	117	31	6	48
CLS$_{90}$	237	-11, 37	118	36	7.64	55
CLS$_{95}$	237	NA[b]	117	32	0.3	61
CLS$_{99}$	237	NA[b]	117	39	NA	76
S$_8$	228	NA[b]	120	51	NA	100

[a] The temperature at which the 5% mass loss was observed. [b] The temperature at the peak maximum of the endothermic melting. [c]The reduction of percent crystallinity of each samples was calculated with respect to sulfur (normalized to 100%)

Table 2. Flexural strengths for lignin-sulfur materials

Materials	Flexural strength/Modulus MPa
CLS$_{80}$	> 3.6[a]/ 248
CLS$_{85}$	> 2.4[a]/ 207
CLS$_{90}$	2.5[b]/ 190
CLS$_{95}$	2.1[b]/ 156
CLS$_{99}$	1.8[b]/ 136
SAL$_{95}$	2.1[b]/ 87

[a] The sample does not break after reaching the maximum stress (10 N) applicable by the DMA instrument, so this number represents a lower limit to the material's strength. [b] The sample broke at its maximum flexural strength.

Incorporating more crosslinking chlorolignin progressively lowers the crystallinity of the resultant material. The diminishing crystallinity corresponds to concomitant increase in the flexibility of the materials as measured by dynamic mechanical analysis (*vide infra*). The possibility of phase separation or the presence of other domains besides sulfur and the crosslinked network material was further ruled out by a combination of X-ray powder diffraction (ESI Figure S11) and scanning electron microscopy with element mapping by energy-dispersive X-ray analysis (SEM-EPS, ESI Figure S14) for all of the materials.

The flexural strengths of **CLS$_x$** composites determined from stress-strain analysis (Figure S8, ESI) significantly exceed that achievable in **SAL$_{95}$** (Table 2). In fact, even **CLS$_{99}$**, containing only 1 wt.% chlorolignin crosslinker, has a flexural strength (1.8 MPa) comparable to that of **SAL$_{95}$** (2.1 MPa). The flexural strength of **CLS$_{80}$** (>3.6 MPa) is nearly identical to that of Portland cement (3.7 MPa) and to the strongest reported cellulose/sulfur composites (up to 3.8 MPa).[18]

Water uptake can be detrimental to mechanical properties of polymers containing polar functional groups like those found in lignin. A familiar example is the precipitous drop in the T_g of nylon-6,6 from 100 °C (dry) to 43 °C upon uptake of 3.5 wt.% water, accompanied by a drop in tensile strength at yield from 80 MPa to 43 MPa.[40] Samples of **CLS$_x$** submerged in water for 24 h, however, absorbed ≤0.5% wt.% water without change in dimensions or mechanical properties (Table S5, ESI). Given that high sulfur-content materials have long served as preeminent acid-resistant cements,[41, 42] a **CLS$_{85}$** sample was also submerged in 0.5 *M* aqueous H_2SO_4 to assess its resistance to acid degradation. Impressively, even after 24 h in the acid, **CLS$_{85}$** retained 100% of its flexural strength (Figure S9 ESI). For comparison, a Portland cement sample of the same dimensions loses all integrity after just 30 minutes in the acid solution. In addition to matching the flexural strength of Portland cement while offering improved acid stability, **CLS$_x$** materials retain full mechanical strength over many pulverization-remelt-recast cycles (Figure S10, ESI), thus demonstrating recyclability unattainable with Portland cement systems.

Given that **CLS$_x$** materials exhibit flexural strength on par with that of ordinary Portland cement (OPC), one potential practical application of these materials could be as more sustainable and recyclable building materials. In this regard, the low thermal conductivity of sulfur (0.269 W m^{-1} K^{-1}) could be an asset, as walls built of **CLS$_x$** cements would be expected to have higher insulation value than traditional cement walls. As a facile demonstration, an architectural model made of 19 mm-thick extruded polystyrene insulation boards was assembled with two ports cut in one of the

walls (Figure 3). One port was covered with a 4.4 mm-thick OPC tile, while the other was covered with a 3.1 mm-thick **CLS$_x$** tile. The exterior temperature (T_{ext}) was 19.9 °C (67.8 °F), while the internal temperature (T_{int}) was raised to 34.2 °C (93.6 °F) by action of a heated electric coil positioned equidistant from the tiles. The temperature breakthrough was monitored using a thermal imaging camera of the type used by building inspectors to test for building insulation leaks. The **CLS$_x$** tile allowed a 5 minute temperature breakthrough value significantly better than that of the OPC tile, despite the **CLS$_x$** tile being only 70% of the thickness of the OPC tile, with the OPC tile's external surface temperature reaching 7.3 °C greater than ambient, whereas the **CLS$_x$** tile's surface temperature was only 4.3 °C greater than ambient (Figure 3B). These data demonstrate that, not only is **CLS$_x$** strong and recyclable, but it also exhibits significantly improved thermal insulative ability in block-build construction over currently-employed OPC installations.

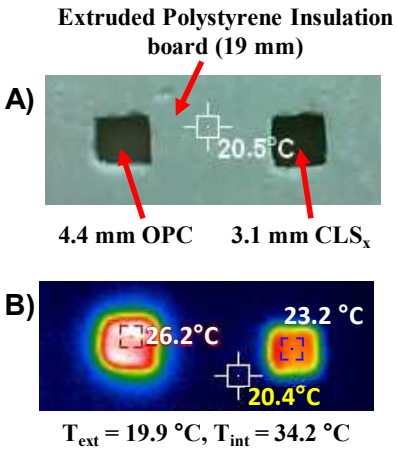

Figure 3. Two ports in the wall of an architectural model are filled with tiles of ordinary Portland cement (OPC, left) or **CLS$_x$** (right). The internal temperature raised to 34.2 °C and the exterior was imaged by an optical camera (A) and a thermal imaging camera (B) to demonstrate the better thermal insulative ability of **CLS$_x$**.

Conclusions

In conclusion, RASP has been demonstrated as a viable route to high sulfur-content materials wherein polymeric sulfur domains are stabilized by a supporting network of sulfur-crosslinked lignin. The RASP methodology thus allows direct reaction of two industrial waste products to prepare **CLS$_x$** composites. **CLS$_x$** composites exhibit flexural strength on par with that of Portland cement, are recyclable over many cycles without loss of mechanical properties by simply melting them down and pouring into molds to cast new shapes. These lignin-sulfur composites also resist challenge by oxidizing acid. Such durable, recyclable, chemically-resistant materials hold promise as elements for lignin valorization and more sustainable building practices.

Conflicts of interest

There are no conflicts to declare

Acknowledgements

Funding for this project from the National Science Foundation (CHE-1708844) is gratefully acknowledged.

Keywords: Chlorolignin • Radical induced polymerization • Lignin-sulfur composites • Polymeric sulfur

Notes and References

1. T. Thiounn, M. K. Lauer, M. S. Bedford, R. C. Smith and A. G. Tennyson, *RCS Advances*, 2018, **8**, 39074-39082.
2. A. D. Smith, T. Thiounn, E. W. Lyles, E. K. Kibler, R. C. Smith and A. G. Tennyson, *Journal of Polymer Science Part A: Polymer Chemistry*, 2019, **57**, 1704-1710.
3. A. Takahashi, R. Goseki, K. Ito and H. Otsuka, *ACS Macro Letters*, 2017, **6**, 1280-1284.
4. M. Arslan, B. Kiskan and Y. Yagci, *Scientific Reports*, 2017, **7**, 5207.
5. A. G. Simmonds, J. J. Griebel, J. Park, K. R. Kim, W. J. Chung, V. P. Oleshko, J. Kim, E. T. Kim, R. S. Glass, C. L. Soles, Y.-E. Sung, K. Char and J. Pyun, *ACS Macro Lett.*, 2014, **3**, 229-232.
6. J. J. Griebel, N. A. Nguyen, S. Namnabat, L. E. Anderson, R. S. Glass, R. A. Norwood, M. E. Mackay, K. Char and J. Pyun, *ACS Macro Letters*, 2015, **4**, 862-866.
7. F. Zhao, Y. Li and W. Feng, *Small Methods*, 2018, **2**, 1-34.
8. M. Mann, J. E. Kruger, F. Andari, J. McErlean, J. R. Gascooke, J. A. Smith, M. J. H. Worthington, C. C. C. McKinley, J. A. Campbell, D. A. Lewis, T. Hasell, M. V. Perkins and J. M. Chalker, *Organic & Biomolecular Chemistry*, 2019, **17**, 1929-1936.
9. S. F. Valle, A. S. Giroto, R. Klaic, G. G. F. Guimaraes and C. Ribeiro, *Polymer Degradation and Stability*, 2019, **162**, 102-105.
10. G. Kutney, *Sulfur. History, Technology, Applications & Industry*, ChemTec, Toronto, 2007.
11. D. J. Parker, S. T. Chong and T. Hasell, *RSC Adv.*, 2018, **8**, 27892-27899.
12. M. J. H. Worthington, R. L. Kucera and J. M. Chalker, *Green Chem.*, 2017, **19**, 2748-2761.
13. D. J. Parker, H. A. Jones, S. Petcher, L. Cervini, J. M. Griffin, R. Akhtar and T. Hasell, *Journal of Materials Chemistry A: Materials for Energy and Sustainability*, 2017, **5**, 11682-11692.
14. W. J. Chung, J. J. Griebel, E. T. Kim, H. Yoon, A. G. Simmonds, H. J. Ji, P. T. Dirlam, R. S. Glass, J. J. Wie, N. A. Nguyen, B. W. Guralnick, J. Park, A. Somogyi, P. Theato, M. E. Mackay, Y.-E. Sung, K. Char and J. Pyun, *Nat Chem*, 2013, **5**, 518-524.
15. Y. Zhang, R. S. Glass, K. Char and J. Pyun, *Polym. Chem.*, 2019, DOI: 10.1039/c9py00636b, Ahead of Print.
16. J. M. Chalker, M. J. H. Worthington, N. A. Lundquist and L. J. Esdaile, *Topics in Current Chemistry*, 2019, **377**, 1-27.
17. M. Karunarathna, M. K. Lauer, T. Thiounn, R. C. Smith and A. G. Tennyson, *Journal of Materials Chemistry A*, 2019, **7**, 15683-15690.
18. M. K. Lauer, T. A. Estrada-Mendoza, C. D. McMillen, G.

Chumanov, A. G. Tennyson and R. C. Smith, *Advanced Sustainable Systems*, 2019, DOI: 10.1002/adsu.201900062.
19. A. D. Macallum, *Journal of Organic Chemistry*, 1948, **13**, 154-159.
20. S. Oae and Y. Tsuchida, *Tetrahedron Letters*, 1972, DOI: 10.1016/s0040-4039(01)84568-8, 1283-1286.
21. P. C. Lindholm-Lehto, J. S. Knuutinen, H. Ahkola and S. H. Herve, *Environmental Science and Pollution Research*, 2015, **22**.
22. L. Zoia, A. Salanti, P. Frigerio and M. Orlandi, *BioResources*, 2014, **9**, 6540-6561.
23. A. Granata and D. S. Argyropoulos, *Journal of Agricultural and Food Chemistry*, 1995, **43**, 1538-1544.
24. D. S. Argyropoulos, *Journal of Wood Chemistry and Technology*, 1994, **14**, 45-63.
25. C. Crestini, H. Lange, M. Sette and D. S. Argyropoulos, *Green Chemistry*, 2017, **19**, 4104-4121.
26. E. F. Mooney, *Spectrochimica Acta*, 1963, **19**, 877-887.
27. H. I. Bolker, H. E. W. Rhodes and K. S. Lee, *Journal of Agricultural and Food Chemistry*, 1977, **25**, 708-716.
28. B. Hortling and J. J. Lindberg, *Makromolekulare Chemie*, 1978, **179**, 1707-1718.
29. D. R. Goud, D. Pardasani, A. K. Purohit, V. Tak and D. K. Dubey, *Analytical Chemistry (Washington, DC, United States)*, 2015, **87**, 6875-6880.
30. K. K. Jena and S. M. Alhassan, *Journal of Applied Polymer Science*, 2016, **133**.
31. D. S. Tarbell and D. P. Harnish, *Chemical Reviews (Washington, DC, United States)*, 1951, **49**, 1-90.
32. D. P. Harnish and D. S. Tarbell, *J. Am. Chem. Soc.*, 1948, **70**, 4123-4127.
33. D. P. Harnish and D. S. Tarbell, *Journal of the American Chemical Society*, 1948, **70**, 4123-4127.
34. P. Eyer, F. Worek, D. Kiderlen, G. Sinko, A. Stuglin, V. Simeon-Rudolf and E. Reiner, *Analytical Biochemistry*, 2003, **312**, 224-227.
35. M. Brebu and C. Vasile, *Cellulose Chemistry and Technology*, 2010, **44**, 353-363.
36. S. Diez, A. Hoefling, P. Theato and W. Pauer, *Polymers (Basel, Switzerland)*, 2017, **9**, 59/51-59/16.
37. K. Bandzierz, L. Reuvekamp, J. Dryzek, W. Dierkes, A. Blume and D. Bielinski, *Materials*, 2016, **9**, 607/601-607/617.
38. A. M. Zaper and J. L. Koenig, *Makromolekulare Chemie*, 1988, **189**, 1239-1251.
39. A. Smith and W. B. Holmes, *Journ. Americ. Chem. Soc.*, 1905, **27**, 979-1013.
40. C. C. Pai, R. J. Jeng, S. J. Grossman and J. C. Huang, *Advances in Polymer Technology*, 1989, **9**, 157-163.
41. H. H. Weber, *American Concrete Institute*, 1993, **SP-137**, 49-72.
42. H. H. Weber and W. C. McBee, Washington, D.C. , 2000.